

Optimization of the adsorption of methyl green dye on almond shells using central composite design

Mehmet Kayra Tanaydin^{a,*}, Ali Goksu^b

^aDepartment of Chemistry and Chemical Processes, Tunceli Vocation School, Munzur University, Tunceli, Turkey, Tel. +90(428) 213 17 94; Fax: +90(428) 213 16 24; email: tanaydinmehmet@gmail.com

^bDepartment of Gastronomy and Culinary Arts, Faculty of Fine Arts, Munzur University, Tunceli, Turkey, email: aligoksu58@hotmail.com

Received 2 October 2019; Accepted 3 April 2021

ABSTRACT

Almond shells, known as the agricultural industry's waste, were utilized to adsorb methyl green dye from aqueous solutions. The effects of initial concentration (2–10 mg/L), the adsorbent dosage (0.1–0.5 g), shaking speed (150–250 rpm), pH (4–7), temperature (20°C–50°C), and particle size (137–892 μm) on methyl green adsorption on the almond shell were examined. The response surface methodology was used to optimize the methyl green dye's adsorption process using the almond shell. The central composite design was utilized to obtain optimum experimental conditions. Performed experiments obtained the isotherm data, and it was analyzed by utilizing the Langmuir, Freundlich, and Temkin isotherm models. The isotherm data can be fitted well by the Langmuir model. The pseudo-second-order model can anticipate the adsorption kinetics. The thermodynamic parameters such as ΔG° , ΔH° , and ΔS° were calculated and found to be -2.878 , 42.12 kJ/mol, and 0.151 kJ/mol K, respectively. These values demonstrated that the present adsorption process was feasible, spontaneous, and endothermic in the temperature scope of (20°C–50°C). This study indicates that almond shells were considered an efficient adsorbent to remove from the aqueous solutions. The maximum adsorption capacity of the almond shell (1.1 mg/g) was obtained. In this system, the almond shell's pre-activation process was not preferred because it will create an extra cost. Adsorption kinetics studies showed that the model is represented as a pseudo-second-order of adsorption data.

Keywords: Almond shells; Methyl green; Central composite design; Adsorption isotherm; Thermodynamics

1. Introduction

A large number of industrial products such as paper, textile, rubber, paint, food, medicine, plastic, and leather use a large number of dyes to color and release their waste to wastewater streams. The release of colored wastewater from these industries can pose an eco-toxic hazard and potentially pose a threat to bioaccumulation [1–3]. These dyes also have good stability against light, heat, and oxidants and it has a higher solubility in water [4]. Therefore, it is essential to investigate the removal of industrial dyes from wastewater

systems. It has been conferred that excessive organic dye intake can damage the digestive tract, the liver, and the central nervous system of the human directly. More than 100,000 dyes exist with different chemical structures available commercially and produce more than 1 million tons of dyes per year, of which 50% are textile dyes [5]. Dyes are classified as cationic, anionic, and nonionic depending on their molecules' ion load [6]. The cationic dye is more toxic than the anionic one. Within the types of dye, methyl green (MG) type is a member of the triphenylmethane-type dicationic dye, and it is used in many different areas such as paper for staining solutions in medicine and biology

* Corresponding author.

textile dyeing, etc. [7,8]. Dyes can be removed using some chemical, physical, and biological treatment methods. The chemical procedure contains such as photolysis and photocatalytic operations, though biological methods involve anaerobic and aerobic degradation and physicochemical methods include ion exchange, electro-kinetic coagulation, membrane filtration, and adsorption [5,9,10]. All techniques have their very own confinement based on cost, design, and dye removing efficiency. In any case, adsorption is the most suitable technique in examination with others in various regards [11]. Among these physical and chemical methods, adsorption is better than others to remove the dyes for its operating cost, ease, inactivity on toxic substances, and anticipate to be promising for a broader scope of compounds than any of the other listed processes [12,13].

Many materials can be used as solid-phase adsorbents to remove dye from water, such as activated carbon, agricultural waste, natural materials, clay, modified clay, coal, polymers, and graphene composites, etc. [4,8,14]. Activated carbon is a practical yet costly adsorbent because of the high costs of manufacturing. It can also not be utilized to treat a vast number of effluents on account of financial thought. On the other hand, there is a developing interest in utilizing low-cost materials for the adsorption of dyes such as almond shell, sunflower seeds, peanut shell, palm, banana peel, lemon peel, papaya seeds, chitosan/oil palm ash, rice husk, and orange peel, etc. are cheap and utilized as low-cost adsorbents instead of activated carbons [12,15–18]. In 2019, almond production in the world was 3.5 million metric tons [19].

In contrast, turkey ranks 4th globally; it took place in the same year by producing 150 thousand tons [20]. In this study, the almond shell without any pre-treatment was used. The reason for this is that almond shells are available locally and are cheap to obtain. Studies on the treated and untreated almond shell with crystal violet [21–23] and methyl violet 2B dyes [24]. In these studies, kinetic, thermodynamic, and isotherm of adsorption were examined.

There is no publication about optimization study of methyl green absorption on almond shell with central composite design (CCD) to the best of the authors' knowledge. This study aims to use almond shells disposed of as waste material of the food industry as a low-cost adsorbent for removing MG from an aqueous solution.

There has been no investigation about the optimization of test conditions by response surface method (RSM) on MG's adsorption by utilizing the almond shell. To advance the adsorption procedure's trial parameters, the consolidated impact of the adsorbent dosage, concentration, pH, and shaking speed is utilized by Design-Expert (State-Ease, Inc., Minneapolis, USA) in a CCD in RSM. RSM is an exact displaying system utilized to decide the connection between a lot of exploratory factors and monitored results. It comprises of three main steps: (1) conducting statistically designed tests, (2) assessing coefficients in a mathematical model, and (3) anticipating the response and controlling the sufficiency of the model. In the present investigation, a five-level variable CCD was used to figure out adsorption process optimization values. Therefore, in this study, CCD was utilized to inspect the optimum adsorption conditions to remove MG dye from the aqueous solution using the almond shell. The composition of the almond shells (before and

after the adsorption) was characterized using Fourier transform infrared spectroscopy (FTIR). Adsorption (Langmuir, Freundlich, and Temkin) isotherms were reported. Also, the kinetics, thermodynamics, and isotherms of the adsorption were discussed. The CCD was used to define optimal conditions for maximizing MG's removal from the aqueous solutions and reduce the overall testing cost and time.

2. Material and methods

2.1. Adsorbent

In this paper, the almonds, gathered from the horticultural zones of Elazig, Turkey, were dried usually, and then pounded to a small size of the almond shells. These shells were grounded and screened through a set of sieves to get distinctive particle dimensions of almond shells and stored. After this procedure, particle diameter (D_p) ranging between $0.8952 > D_p > 0.137$ mm was acquired and utilized without any further pre-treatment.

2.2. Adsorbate solution

Analytical grade MG was purchased from Sigma-Aldrich, Germany (MERCK). One liter of 100 ppm stock solution of MG was set up by dissolving 0.1 g of the MG with ultrapure deionized water (UPDIW) (Purelab Flex). The necessary amount was taken from the stock solution and diluted with UPDIW to set up the desired concentration (2, 4, 6, 8, and 10 ppm). The dye solution's pH was adjusted by using 0.1 M NaOH or/and 0.1 M HCl.

2.3. Methyl green adsorption studies

The removal tests were carried out in a 100 mL Erlenmeyer flask, and the volume of the batch reactor was kept at 50 mL. The effects of different operating parameters like pH (4–7), temperature (20°C–50°C), contact time (5–180 min), initial concentration (2–10 ppm), adsorbent dosage (0.1–0.5 g), and shaking speed (150–250 rpm) on the adsorption were observed. After every adsorption procedure, samples were pulled back at various time intervals. The supernatant was expelled from the solutions by utilizing a centrifuge for 5 min at 5,000 rpm. The samples at initial time = 0 and each time interval were analyzed using a double beam UV-VIS spectrophotometer at 632 nm (Shimadzu, Model, Japan). The amount of adsorption after equilibrium was calculated by:

$$q_e = \frac{(C_0 - C_e)V}{W} \quad (1)$$

where C_0 and C_e (mg/L) are the initial and equilibrium concentration of the MG, respectively. V is the volume of the liquid phase solution (L), and W is the weight of utilized dry adsorbate (g).

The percentage of MG removal from the solution was calculated as follows:

$$\text{Removal percentage} = \frac{(C_0 - C_e)}{C_0} \times 100 \quad (2)$$

2.4. Experimental design

The application of classical experimental design methods is complex and challenging. These techniques likewise require countless experiments related to an expanding number of parameters. The response surface method is an appropriate method to reduce the number of experiments and determine the optimal experimental parameters.

RSM is a collection of statistical and mathematical methods that are valuable for investigating the effect of a few independent parameters on the response and placing empirical models in experimental data. The primary objective of RSM is to establish the connection between a set of test parameters and monitored results. RSM consists of the following advances: (i) doing statistically designed tests, (ii) to estimate coefficients in the scientific model, and (iii) to estimate the answer and checking the sufficiency of the model [25,26].

A five-level four-factor CCD was employed, requiring 30 experimental runs (calculated based on Eq. (3)), which consist of eight axial runs, 16 factorial runs, six replicate runs at the center:

$$N = 2^n + 2n + N_c = 2^4 + 2 \times 4 + 6 = 30 \tag{3}$$

where N is the total experimental runs and n is the number of variables.

An empirical model has been developed to relate based on the quadratic second-order-model for removing MG using almond shells given by Eq. (4) to respond to the adsorption process and analyze the effect of parameter interactions:

$$Y = \beta_0 + \sum_{i=1}^k \beta_i x_i + \sum_{i=1}^k \sum_{j=1}^k \beta_{ij} x_i x_j + \sum_{i=1}^k \beta_{ii} x_i^2 + \epsilon \tag{4}$$

where Y is the measured response; β_0 is the intercept; β_i , β_{ij} and β_{ii} are coefficients of the linear effect, double interactions; ϵ is the error; and x_i , x_j are the independent variables or factors.

3. Results and discussion

One of the principal goals of RSM is to figure out the optimum settings of control factors that cause a maximum response. This requires a decent fitting model that gives a satisfactory representation of the average response because such a model will be utilized to find the value of the optimum. The optimization methods utilized in RSM rely upon the nature of the fitted model [27]. In Fig. 1, the black line expresses the spectrum of methyl green before the adsorption, and the red line shows the spectrum of it after adsorption.

In the present examination, to optimize the removal of MG by an adsorption process, essential parameters are given in Table 1, initial concentration (A), adsorbent dosage (B), pH (C), and time (D) were taken into consideration. As a result, while A , B , C , and D were picked as independent variables, the removal of (Y) MG in equilibrium was chosen as the study's response (dependent variable). The experimental removal efficiency (%) for MG dye can be seen in Table 2. The final CCD obtained for the removal of MG as a percentage with significant terms is quadratic as recommended by the software and is given as follows:

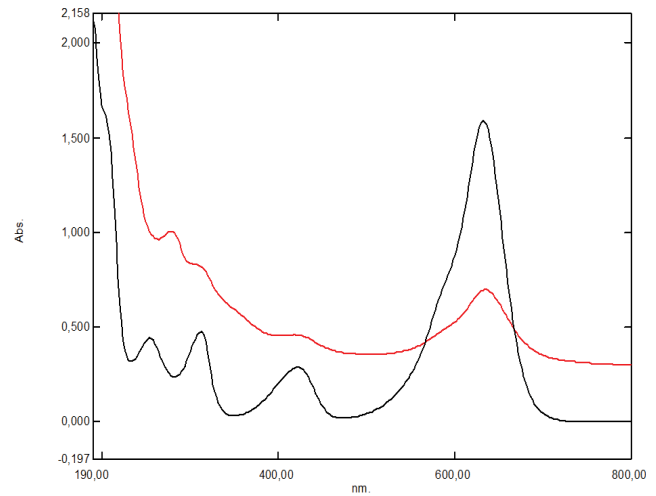


Fig. 1. Spectrum of methyl green before and after adsorption.

Table 1
Variables and levels are considered for a percentage of removal of MG

Parameters	Low	High
Initial concentration (A), mg/L	4	8
Adsorbent dosage (B), g	0.2	0.5
pH (C)	4	7
Time (D), min	40	100

$$\begin{aligned} \text{Removal MG \%} = & +77.84 - 5.708 \times A + 25.292 \times B - 0.542 \\ & \times C + 3.042 \times D + 2.313 \times AB - 2.062 \times AC + 1.937 \\ & \times AD + 0.315 \times BC + 2.313 \times BD - 0.563 \times CD - 1.135 \\ & \times A^2 - 6.261 \times B^2 - 0.635 \times C^2 - 2.01 \times D^2 \end{aligned} \tag{5}$$

Eq. (5) demonstrates how singular variables are (quadratic) or binary interaction, affecting MG's removal from the aqueous solution with the almond shell as an adsorbent. Negative coefficient values indicate that the singular or pairs of interacting factors that negatively affect MG adsorption (i.e., adsorption percentage decreases); whereas, positive coefficient values mean that the tested range of factors increases the adsorption MG [28].

The importance of every coefficient for removing MG dye by the almond shell was detected by F and p -values as listed in Table 3. To comprehend the pattern of interactions between parameters were used to test the values in Table 3. Based on these results in Table 3, the relation between the percent removal of MG dye and the selected factors was expressed by the second-order polynomial equation.

The analysis of variance (ANOVA) was utilized to verify the model given in Table 4 to remove MG dye's efficiency using the almond shell. The second-order polynomial analysis and quadratic model were utilized to determine the connection between factors and responses. The F -value of the model ought to be higher than the F -distribution's tabulated value for a certain degree of significance, $\alpha = 5\%$.

Table 2
Experimental design matrix using central composite design

Run	Concentration (ppm)	Adsorbent dosage (g)	pH	Time (min)	MG removal, Y_{MG} (%)
1	2	0.35	5.5	70	86
2	6	0.35	5.5	70	77
3	6	0.05	5.5	70	8
4	6	0.35	8.5	70	80
5	8	0.2	7	40	30
6	6	0.35	5.5	10	58
7	4	0.2	7	40	53
8	6	0.35	5.5	70	80
9	4	0.2	7	100	48
10	8	0.2	4	100	41
11	8	0.2	7	100	24
12	4	0.2	4	40	47
13	10	0.35	5.5	70	62
14	6	0.35	5.5	70	75
15	4	0.5	4	40	99
16	6	0.35	2.5	70	72
17	8	0.2	4	40	37
18	8	0.5	4	100	99
19	8	0.5	7	40	81
20	6	0.35	5.5	130	83
21	4	0.5	7	40	95
22	4	0.5	4	100	98
23	8	0.5	4	40	86
24	4	0.2	4	100	47
25	6	0.35	5.5	70	74
26	6	0.35	5.5	70	76
27	8	0.5	7	100	97
28	6	0.65	5.5	70	99
29	6	0.35	5.5	70	85
30	4	0.5	7	100	97

F -values of the removed percentage of MG by almond shell were accounted for like 8.52, and this value is significant.

The p -values of the model were significant for the removal of MG dye. The insignificant lack of fit, the p -value of 0.1659 for the adsorption of MG dye (p -value is more than 0.05) with almond shell, showed that the quadratic model was substantial for the present investigation.

The high R^2 value indicates that quadratic equations can represent the system under the given experimental field. This is also evident from the predicted and observed values graph for Y_{Cu} in Fig. 2. The predicted data and actual data confirm the relevant results, as shown in Fig. 2.

Fig. 3 shows a three-dimensional surface plot of the empirical model for MG adsorption as a function of the four factors. As shown in Figs. 3a and b, the removal of MG increase with increasing adsorbent dosage and decreases with increasing MG concentration. The increase in adsorbent dosage prompts increasing active adsorption sites. Moreover, as can be seen from Eq. (5), the positive value of adsorbent dosage ($25.292 \times B$) indicated that increasing adsorbent dosage increases MG adsorption dye. The highest

MG removal was obtained when the adsorbent dosage amount was maximum and the concentration was minimum values. Eq. (5) indicated this could be affirmed by the negative value acquired for initial MG dye concentration ($-5,708 \times A$), which indicated that MG's adsorption is inversely proportional to the initial MG dye concentration. Diminishing MG removal (%) with increasing initial MG dye concentration is presumably ascribed to the saturation of active sites on the almond shell's surface. This outcome can likewise be ascribed to the aggregation of MG dye molecules at high concentrations, making it difficult to diffuse into the adsorbent structure. It can be seen from Figs. 3c, d, and f show that changing pH caused no critical effect on the removal of MG%. The effect of pH (F -value: 0.22) produced a slight effect on the adsorption of MG.

Additionally, as can be seen from Eq. (5), the negative value of pH ($-0.542 \times C$) demonstrated that increasing temperature causes a slight drop in MG adsorption. Besides, as it is clear from Figs. 3b, e, and f, increasing adsorption time increased the removal of MG dye adsorption. According to Eq. (5), this result can be confirmed by the positive value

Table 3
Analysis of variance (ANOVA) for response surface quadratic model of MG by adsorption

Source	Sum of squares	df	Mean square	F-value	p-value	Prob. > F
Model	17,784.05	14	1,270.29	38.83	<0.0001	Significant
A-Concentration	782.04	1	782.04	23.90	0.0002	
B-Adsorbent dosage	15,352.04	1	15,352.04	469.24	<0.0001	
C-pH	7.04	1	7.04	0.22	0.6494	
D-Time	222.04	1	222.04	6.79	0.0199	
AB	85.56	1	85.56	2.62	0.1267	
AC	68.06	1	68.06	2.08	0.1698	
AD	60.06	1	60.06	1.84	0.1955	
BC	1.56	1	1.56	0.048	0.8300	
BD	85.56	1	85.56	2.62	0.1267	
CD	5.06	1	5.06	0.15	0.6996	
A ²	35.36	1	35.36	1.08	0.3150	
B ²	1,075.00	1	1,075.00	32.86	<0.0001	
C ²	11.07	1	11.07	0.34	0.5693	
D ²	110.86	1	110.86	3.39	0.0855	
Residual	490.75	15	32.72			
Lack of fit	407.92	10	40.79	2.46	0.1659	Not significant
Pure error	82.83	5	16.57			
Cor. total	18,274.80	29				

Table 4
Fit summary for MG dye removal (%) using the almond shell

Sequential model sum of squares						
Source	Sum of squares	df	Mean square	F-value	p-value	Prob. > F
Mean vs. total	1.462E+005	1	1.462E+005			
Linear vs. mean	16,363.17	4	4,090.79	53.50	<0.0001	
2FI vs. linear	305.88	6	50.98	0.60	0.7245	
Quadratic vs. 2FI	1,115.01	4	278.75	8.52	0.0009	Suggested
Cubic vs. Quadratic	400.33	8	50.04	3.87	0.0455	Aliased
Residual	90.42	7	12.92			
Total	1.644E+005	30	5,481.20			
Lack of fit tests						
Source	Sum of squares	df	Mean square	F-value	p-value	Prob. > F
Linear	1,828.80	20	91.44	5.52	0.0335	
2FI	1,522.92	14	108.78	6.57	0.0241	
Quadratic	407.92	10	40.79	2.46	0.1659	Suggested
Cubic	7.58	2	3.79	0.23	0.8033	Aliased
Pure error	82.83	5	16.57			
Model summary statistics						
Source	Standard deviation	R-squared	Adjusted R-squared	Predicted R-squared	PRESS	
Linear	8.74	0.8954	0.8787	0.8492	2,755.51	
2FI	9.19	0.9121	0.8659	0.8091	3,488.84	
Quadratic	5.72	0.9731	0.9481	0.8649	2,468.88	Suggested
Cubic	3.59	0.9951	0.9795	0.9337	1,211.28	Aliased

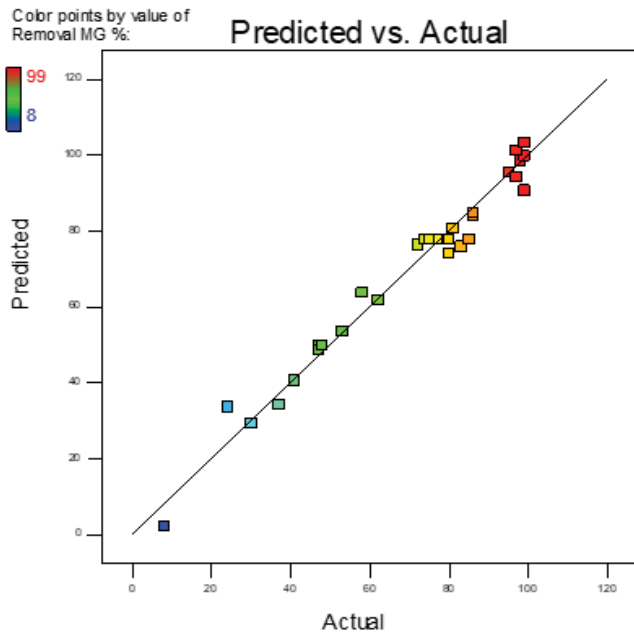


Fig. 2. Predicted vs. actual values plots for MG adsorption.

obtained for adsorption time ($3.042 \times D$) [29–31]. Fig. 3 shows that adsorbent dosage, concentration, and time are effective parameters for removing MG from the aqueous solution.

3.1. Effect of the optimum adsorbent dosage

The effect of the optimum amount of adsorbent was examined at a fixed stirring speed of 200 rpm and a temperature of 20°C for various initial dye concentrations such as 2, 4, 6, 8, and 10 ppm for 24 h. As shown in Fig. 4, the percentage of MG removal increased as the amount of adsorbent increased. This is because the usability of the active sites is emphatically identified with the amount of adsorbent dosage. Meanwhile, the adsorption limit diminished as the adsorption dose increments, and it achieved the optimum adsorption value at 0.5 g. This is probably the consequence of aggregation or covering of the adsorption sites, resulting in a decrease of the accessible surface zone in the dye ions. As shown in Fig. 6, the optimum amount of adsorbent value was selected as 0.5 g and utilized in subsequent experiments.

3.2. Effect of pH on MG adsorption

To demonstrate the effect of the initial pH of solution on adsorption experiments, pH was examined in the vary of pH 4–7. Tests were performed at a temperature of 20°C, adsorbent dosage 0.5 g, an initial concentration between 2–10 ppm and 200 rpm at a stirring speed of 24 h. The effects of pH on MG adsorption and different time scales for 24 h are shown in Fig. 5. Further experiments were performed under the same conditions to determine the effects of pH change over time and were continuously monitored for 0–180 min and shown in Fig. 8. According to Figs. 5 and 6, the adsorption of MG onto the almond shells increases with the increasing pH value of the solutions. This is possibly the aftereffect of dye cations and H⁺ ions, which

were vying for the adsorption sites at lower pH value of the solutions, as proposed in prior investigations [32,33]. On the contrary, almond shells' surface area may have adversely charged on higher pH that will increase the number of dye cations on the surface by electrostatic attraction, as referenced in previous examinations [34,35].

3.3. Effect of the initial concentration of MG solution

To test the effects of initial MG dye concentration on adsorption experiments, the concentration changed in the scope of 2–10 ppm at constant adsorbent dosage 0.5 g, temperature 20°C, and shaking speed at 200 rpm. According to the National Environmental Protection Agency (NEPA), the permissible aromatic concentration in surface waters should be less than 1.0 µg/L [36]. Therefore, we choose the initial concentration of solution 2–10 ppm. As seen in Fig. 7, the removal dye percentage was changed with the initial concentration, and the amount of dye adsorbent on almond shells incremented with the increasing initial concentration of MG while the percentages of the dye adsorption were decreased for the per unit mass of the adsorbent. This may be founded on the increasing concentration caused by the increasing driving force between the aqueous and solid phases and the increasing amount of collisions between dye molecules and adsorbent particles [37].

3.4. Effect of the shaking speed

The tests investigated the effect of shaking speed on the adsorption of MG dye performed in the ranges of 150, 175, 200, 225, and 250 rpm while keeping other parameters constant as temperature, adsorbent dosage, initial concentration, and natural pH of the solutions. Fig. 8 shows the adsorption of the dye increases considerably when the shaking speed increases. It means that the agitation of the dye solution facilitates the dye's diffusion to the outer surface of the particle of the almond shell by providing a reduction in the thickness of the diffusion layer formed around the almond shell [38].

3.5. Effect of the temperature

To examine the effect of the temperature on adsorption, the experiments carried out at a temperature of 20°C, 30°C, 40°C, and 50°C. In these tests, other parameters were constant as adsorbent dose, initial concentration, and shaking speed. The temperature effect is seen in Fig. 9; the percentage of dye removal rising with changing temperature from 20°C to 50°C. This examination demonstrates that the dye's removal increases with temperature, and hence the system is endothermically characterized. The increase in temperature results in increased portability of dye molecules, prompting increased penetration of adsorbent pores [39,40].

3.6. Effect of the particle size

Several experiments were led to determine the effect of particle size on dye adsorption. The almond shell particles were divided in the variety of 137–892 µm and utilized in the trials while different parameters were kept constant

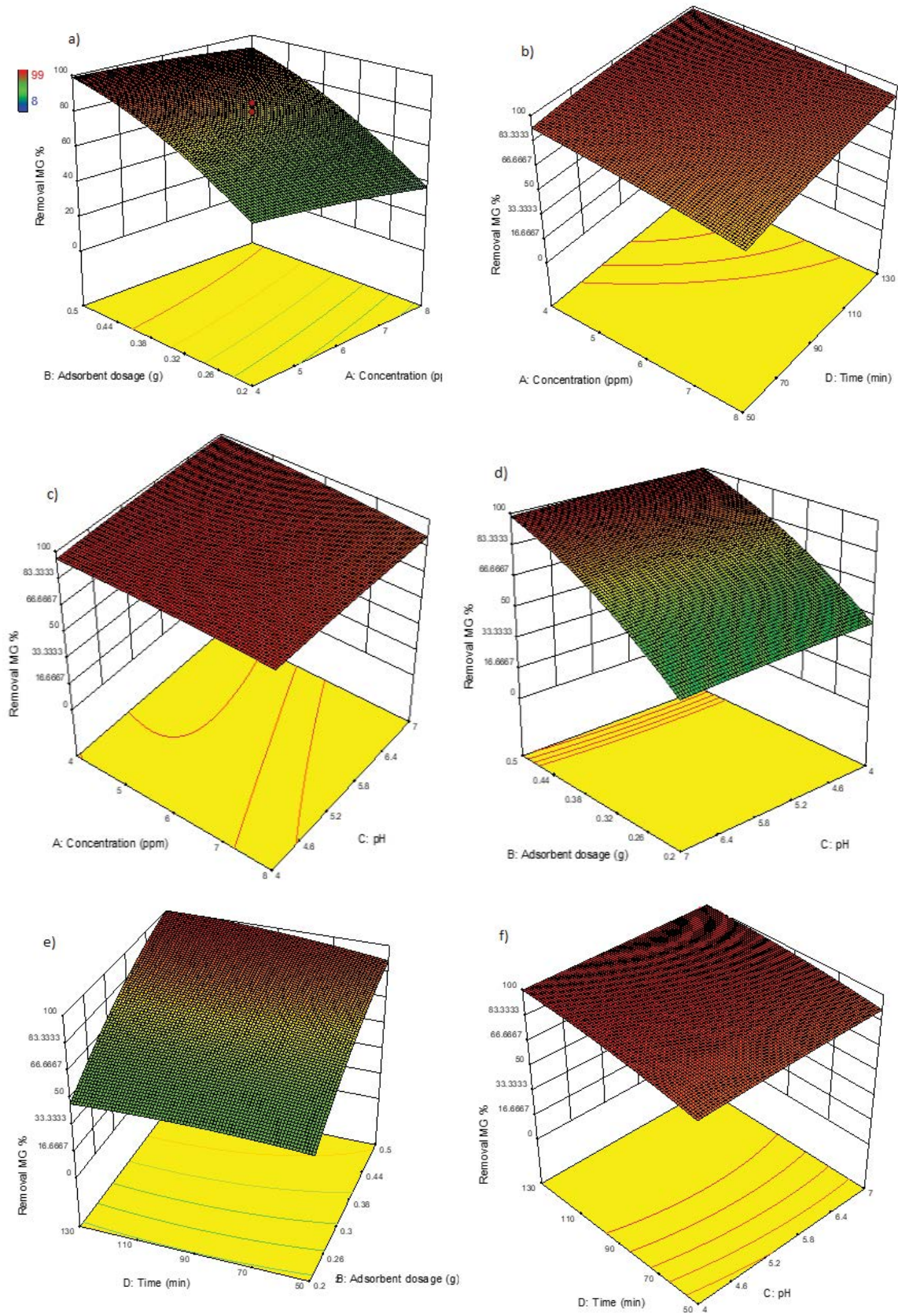


Fig. 3. Response surface graphs (a) adsorbent dosage and concentration, (b) concentration and time, (c) concentration and pH, (d) adsorbent dosage and pH, (e) time and adsorbent dosage, and (f) time and pH on the adsorption of MG.

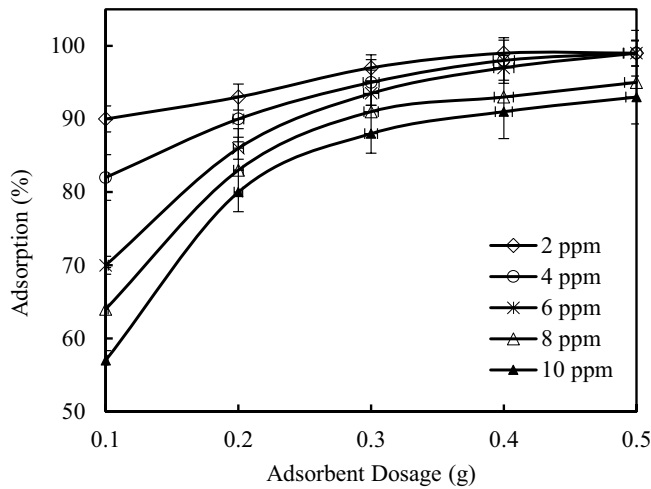


Fig. 4. Effect of adsorbent dosage on MG adsorption.

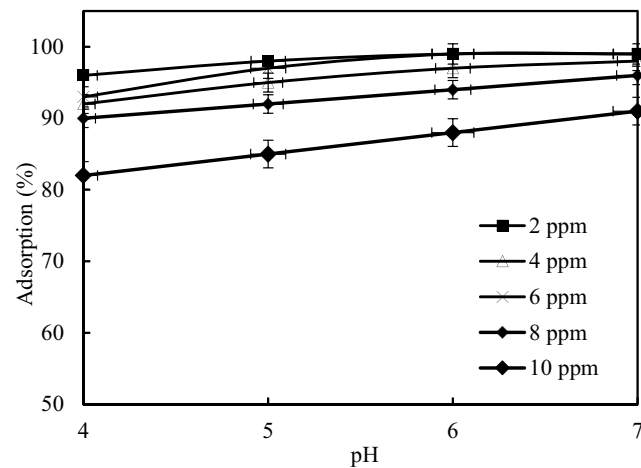


Fig. 5. Effect of initial pH on MG adsorption.

such as adsorbent dosage, stirring speed, and temperature. As shown in Fig. 10, the dye adsorption on the almond shells is increased due to the adsorbent's declining particle size. The adsorbent having a thinner particle size has a higher adsorption capacity than the coarse particle size for dye adsorption because of the greater surface area [41,42].

3.7. Adsorption isotherms

The adsorption equilibrium isotherms are essential for the design and optimization of the adsorption system to remove MG dye molecules from the aqueous solution. The isotherms could be utilized to estimate the interaction between adsorbate and adsorbent [43]. In this examination, the equilibrium data were analyzed by Langmuir, Freundlich, and Temkin isotherms, and the characteristic parameters of each isotherm were calculated and classified in Table 5. The Langmuir isotherm theory recommends that there is monolayer adsorption on a homogeneous external surface adsorbent and that when a dye molecule captures a place, it can no longer possess molecules anymore in the

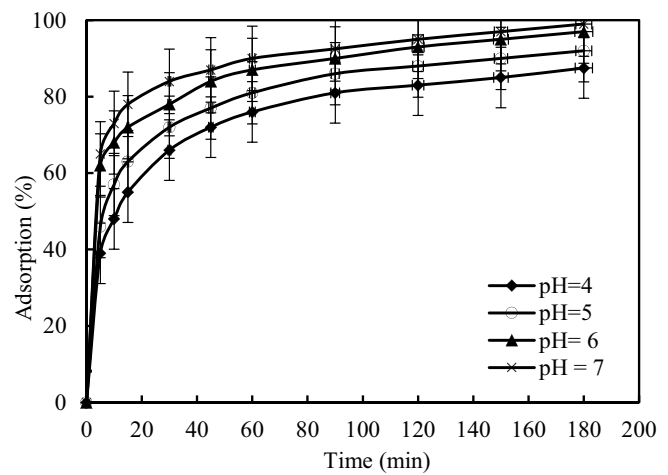


Fig. 6. Effect of initial pH on MG adsorption for various contact time.

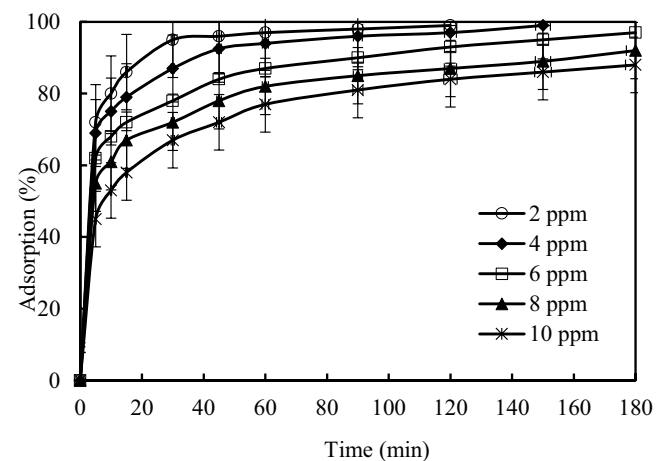


Fig. 7. Effect of initial concentration on MG adsorption for various contact time.

same site [44]. The Freundlich isotherm model is an experimental expression assuming that the surface of the adsorbent is heterogeneous and an exponential distribution of regions and energies [45]. The Temkin model suggests that adsorption's heat will decrease directly with a rising thickness in the adsorbent [11]. The linear equation of Langmuir, Freundlich, and Temkin models [12], individually were:

$$\frac{1}{q_e} = \frac{1}{q_{\max} K_L C_e} + \frac{1}{q_{\max}} \quad (6)$$

$$\ln q_e = \ln K_F + \frac{1}{n} \ln C_e \quad (7)$$

$$q_e = B \ln A + B \ln C_e \quad (8)$$

In the equations above, q_e is the amount of dye adsorbed at equilibrium (mg/g), q_{\max} is the maximum adsorption capacity (mg/g), K_L is the Langmuir constant relation with the energy of adsorption, C_e is the equilibrium concentration

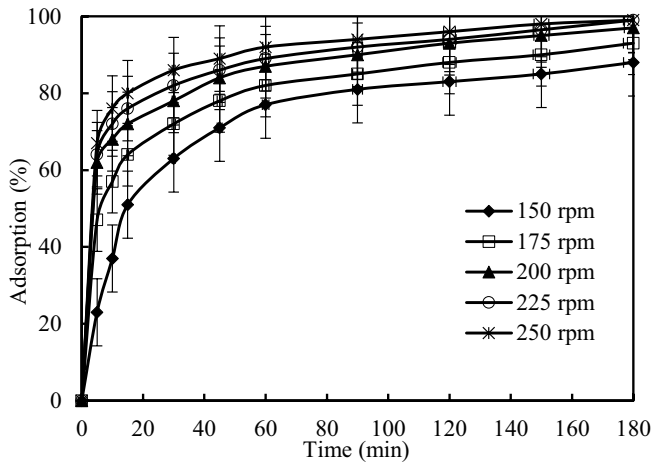


Fig. 8. Effect of shaking speed on MG adsorption for various contact time.

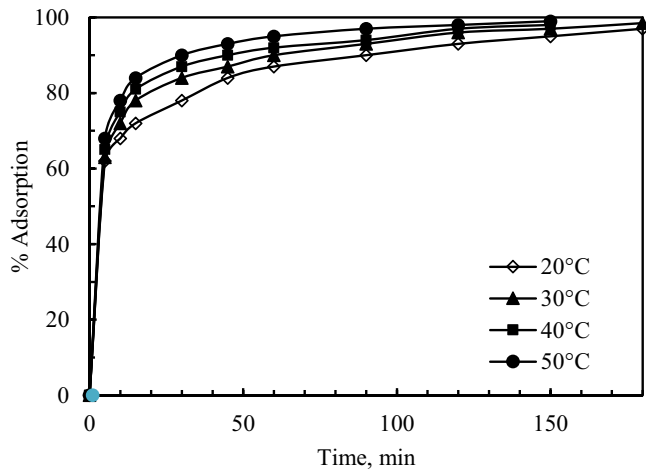


Fig. 9. Effect of temperature on MG adsorption for various contact time.

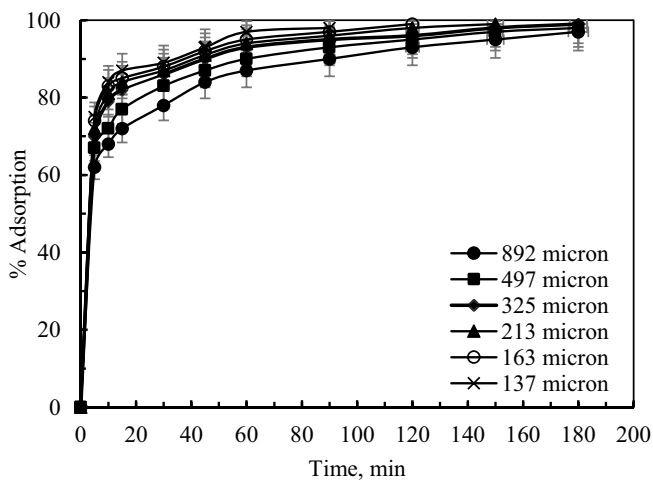


Fig. 10. Effect of the particle size on MG adsorption for various contact time.

(mg/L), K_F is the Freundlich constant relation to adsorption capacity, $1/n$ is the binding strength heterogeneity factors, A is a constant of Temkin isotherm (L/g), B concerns the heat of adsorption (J/mol). The linearized Langmuir isotherm of the dye is given in Fig. 11, respectively. The linear plot of $1/q_e$ vs. $1/C_e$ shows that the adsorption model is well-fitted with the Langmuir model. The Langmuir constants q_{max} and K_L were figured out from the slope and intercepts of the plot, respectively.

The fundamental component of the Langmuir isotherm is affirmed with dimensionless equilibrium parameter (R_L) is given by:

$$R_L = \frac{1}{1 + K_L C_0} \quad (9)$$

In Eq. (9), K_L is the Langmuir constant and C_0 is the highest initial dye concentration (mg/L). The value of R_L shows the category of isotherm accordingly:

- $R_L > 1$ unfavorable adsorption
- $0 < R_L < 1$ favorable adsorption
- $R_L = 1$ linear adsorption
- $R_L = 0$ irreversible adsorption

The R_L values were calculated to be 0.0379, 0.0193, 0.0130, 0.0098, and 0.0078 for the initial concentration of 2, 4, 6, 8, and 10 ppm, respectively. It is confirming that the adsorption of MG on almond shells favorable [46]. The plot of $\ln q_e$ vs. $\ln C_e$ was examined to find out the relevance of the Freundlich isotherm model. The slope ($1/n$) of the plot, is ranging from 0 and 1, is an intensity level of the adsorption or surface heterogeneity. When the value of $1/n$ is closer to zero, it becomes more heterogeneous and when the value goes to closer 1 to, it expresses that cooperative adsorption. The value of B and A could be determined from the plot of q_e vs. $\ln C_e$. The Temkin isotherm model proposes that the heat of adsorption of all molecules in the layer goes down linearly with the coverage based on the interaction between the adsorbent–adsorbate [6].

3.8. Thermodynamics of adsorption

The increasing adsorption rate of the dye along with increasing temperature expresses that the process was endothermic and could be explained by utilizing the parameters of thermodynamics such as; standard free energy change (ΔG°), enthalpy change (ΔH°), and entropy change (ΔS°). These parameters were calculated by using the equations below [47]:

$$K_D = \frac{C_{ac}}{C_e} \quad (10)$$

$$\Delta G^\circ = -RT \ln K_D \quad (11)$$

$$\Delta G^\circ = \Delta H^\circ - T\Delta S^\circ \quad (12)$$

Rearranging Eqs. (11) and (12) is used to obtain the linear form of the following equation:

Table 5
Langmuir, Freundlich, and Temkin isotherm parameters and correlation coefficients for MG adsorption on the almond shell

q_{\max}	Langmuir		Freundlich			Temkin		
	K_L	R^2	K_F	n	R^2	A	B	R^2
1.143	12.68	0.995	1.044	3.443	0.9157	280.26	0.1875	0.98

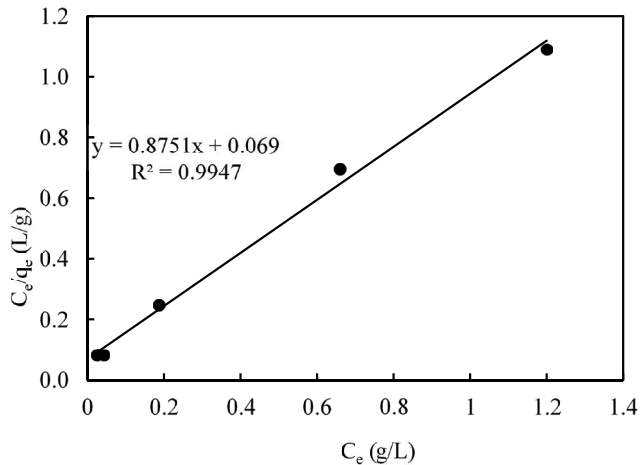


Fig. 11. Langmuir isotherm plot for MG adsorption on the almond shell.

$$\ln K_D = \left(\frac{\Delta S^\circ}{R} \right) - \left(\frac{\Delta H^\circ}{RT} \right) \quad (13)$$

It is called Van't Hoff equation, where K_D is the equilibrium constant, C_{ac} and C_e are the concentration of dye on the adsorbent for the solution (mg/L) at equilibrium, respectively. R is the universal gas constant (8.314 J/mol K), and T is the temperature (K).

The intersection and slope of the linear plot of $\ln K_D$ vs. $1/T$ provide the value of ΔS° and ΔH° , respectively. Additionally, ΔG° can be determined using Eq. (12) for different temperatures and values presented in Table 6. The positive value of ΔH° indicates that the nature of the adsorption process is endothermic. The positive value of ΔS° indicates that the analogy of adsorbent and states the increased randomness at solute–solution interface [47]. The negative value of ΔG° comments that the process is spontaneous and the feasibility of dye adsorption [48,49]. The intersection and slope of the linear plot of $\ln K_D$ vs. $1/T$ give ΔS° and ΔH° , respectively, and the values were given in Table 6. Furthermore, ΔG° can be calculated by Eq. (12)

Table 6
Parameters of thermodynamics for the adsorption of MG on the almond shell

Initial concentration, ppm	ΔH , kJ/mol	ΔS , kJ/mol K	$-\Delta G$, kJ/mol			
			298 K	303 K	313 K	323 K
6	42.12	0.151	2.878	3.633	4.843	6.653

for different temperatures such as 298, 303, 313, and 323 K, and the values can be seen in Table 6.

3.9. Adsorption kinetics

The kinetic data of adsorption can be evaluated to find the dynamics of the adsorption reaction in the rate constant because the kinetic parameters provide essential information to model and design the adsorption process [50]. To evaluate the adsorption kinetics data, pseudo-first and pseudo-second-order kinetic models were applied.

The following equation expresses the linear pseudo-first-order equation:

$$\log(q_e - q_t) = \log q_e - \frac{k_1 t}{2.303} \quad (14)$$

where q_e is the amount of dye adsorbed (mg/g) at equilibrium and k_1 is the first-order reaction rate constant (1/min). q_e and k_1 are calculated by using the intercept and slope, respectively, of the plot of $\log(q_e - q_t)$ vs. t are given in Fig. 12, which has a linear relationship [17].

The linear following equation gives the pseudo-second-order equation:

$$\frac{t}{q_t} = \frac{1}{k_2 q_e^2} + \frac{t}{q_e} \quad (15)$$

where k_2 is the second-order reaction rate constant (g/mg min). A plot of t/q_t vs. t as seen in Fig. 13 shows a linear relationship, and the slope and intercept of the plot give the value of q_e and k_2 , respectively [51]. The results that fitting experimental values with the first and second-order model are illustrated in Table 7. Concerning the data in Table 7, the correlation coefficients (R^2) of the second-order model surpassed 0.99 and q_e values of the second-order model were more acceptable with experimental data than the first-order model. As a result, the adsorption kinetics could be described better with the second-order model than the first-order model.

3.10. Adsorption mechanism

Using the pseudo-first-order and pseudo-second-order kinetic models, the adsorption mechanism could not be

Table 7
Comparison of the kinetic parameters for different initial concentration of MG

Initial concentration (mg/L)	$q_{e,exp}$ (mg/g)	Pseudo-first-order kinetic model			Pseudo-second-order kinetic model		
		k_1 (1/h)	$q_{e,cal}$ (mg/g)	R^2	k_2 (g/mg h)	$q_{e,cal}$ (mg/g)	R^2
2	0.245	0.0320	0.058	0.828	2.424	0.205	0.999
4	0.48	0.0242	0.144	0.894	0.848	0.399	0.999
6	0.70725	0.0209	0.255	0.919	0.304	0.587	0.998
8	0.915	0.0188	0.331	0.902	0.243	0.740	0.997
10	1.075	0.0163	0.420	0.871	0.194	0.924	0.997

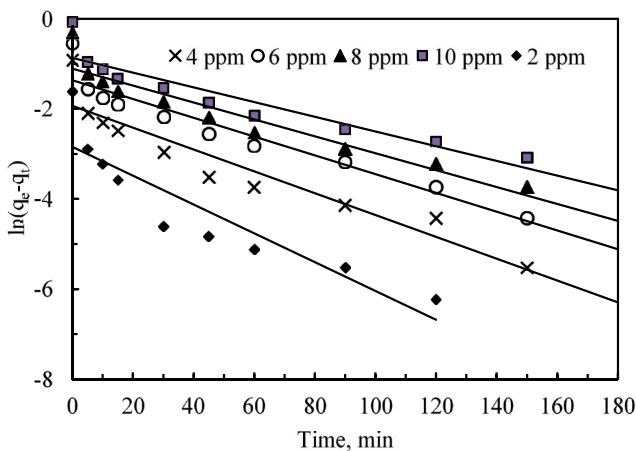


Fig. 12. Pseudo-first-order kinetic for MG on the almond shell.

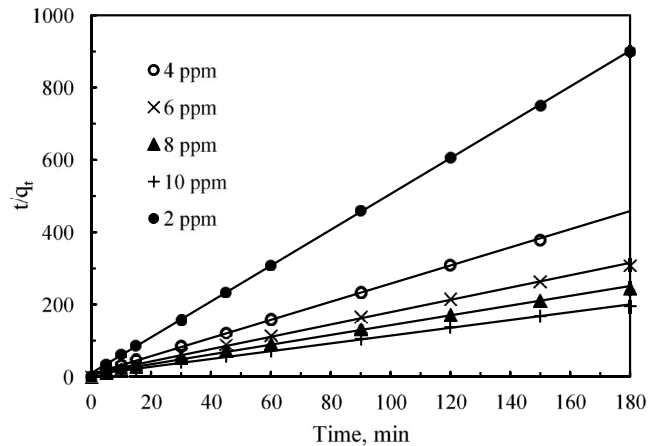


Fig. 13. Pseudo-second-order kinetic model for MG adsorption.

identified; for this reason, the kinetic results were examined utilizing the intra-particle-diffusion model [52]. The adsorption mechanism is generally sectionalized into the following steps [53]:

- MG molecules are transferred from an aqueous solution to the boundary layer surrounding the adsorbent, known as bulk diffusion.
- Transfer of MG molecules in boundary film to the outside surface of sorbent through the process known as film diffusion.
- Transport of the MG molecules from the surface to intra-particle active sites, through the process, is known as intra-particle diffusion.
- Adsorption of the MG molecules by the active sides of the adsorbent.

The first and last steps do not include rate control steps. Hence, the first step is not related to the adsorbent, and the last step is a fast operation. For that reason, film and intra-particle diffusion are primarily connected to the rate-controlling steps. The Weber and Morris intraparticle diffusion model is generally utilized to estimate the rate of controlling steps. The intra-particle diffusion equation can be written by the following equation [54]:

$$q_t = k_{id}t^{1/2} + C \quad (16)$$

where k_{id} (mg/g min^{1/2}) is the intra-particle diffusion constant, C is the thickness of the boundary layer, q_t is the amount of adsorbed MG on time t and, $t^{1/2}$ is the square root of the time. If the graph of q_t vs. $t^{1/2}$ in Fig. 14 gives a straight line, then the adsorption process would be controlled with the intra-particle-diffusion model, and the k_{id} and C can be determined by the slope and intercept of the plot, respectively. However, if the data display multilinear plots, then the first sharper component shows the external surface adsorption, also noted as the instantaneous adsorption stage. The more extensive slopes of the primary component infer that the adsorption rate is very high at the initial time relies upon lots of surface zone and active adsorption sites. The second sharp component suggests that the gradual adsorption stage where the intraparticle diffusion is the rate controlled. The lower slopes of the second component demonstrate that the diffusion of MG molecules on the micropores of adsorbent takes a long time because of the diminished concentration profile. For other cases, the third component's stifled slopes could be showed up that it demonstrates the final equilibrium stage. For this stage, intra-particle diffusion starts gradually down due to the deficient adsorbate concentration left in the bulk solution [55].

3.11. FTIR spectroscopy study

The FTIR spectral evaluation is vital to apprehend the functional groups which might be accountable for adsorption.

The evaluation of FTIR spectra for MG and MG-almond shells turned into illustrated in Fig. 15. The wideband at $3,419\text{ cm}^{-1}$ may be performed that the existence of $-\text{OH}$ and $-\text{NH}$ groups on the surface of the adsorbent, shifting to $3,421\text{ cm}^{-1}$ after MG are adsorbed onto the surface of the adsorbent. The absorption band at $2,921$ represents a typical deformation vibration of the $-\text{CH}$ group. The band at $1,744$ is related to the stretching vibration of $\text{C}=\text{O}$ groups [56,57]. The bands at $1,617.89$ and $1,508$ are associated with stretching vibration of $\text{C}=\text{C}$ functional groups bending. The band at $1,384\text{ cm}^{-1}$ was due to $\text{C}-\text{C}$ aromatic stretching. The absorption bands at $1,252$ and $1,049\text{ cm}^{-1}$ confirm the functional groups $\text{C}-\text{C}$, $\text{C}-\text{H}$ bending, respectively [13,58]. Another three adsorption bands were seen at $1,049$ and 617 due to the sulphonic group and $\text{C}-\text{S}$ stretching vibration, respectively [59]. The peak at $1,252$ may be from the stretching vibration of $\text{C}-\text{O}$ in phenols

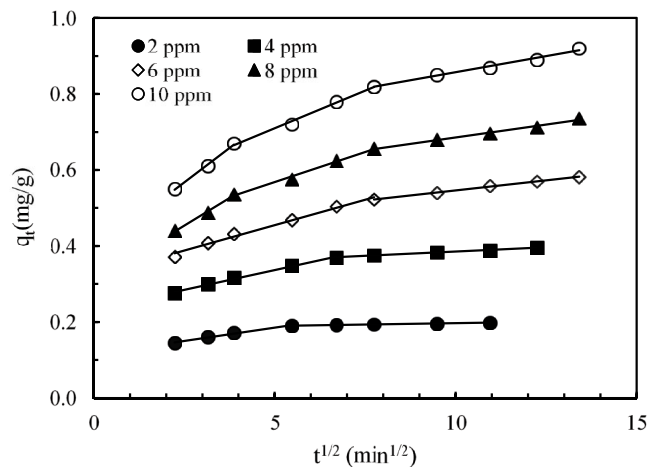


Fig. 14. Intra-particle diffusion model for the adsorption of MG onto the almond shell.

[60]. The peaks at $500\text{--}1,500\text{ cm}^{-1}$ may be the aromatic region related to the ligneous components [61]. The characteristic band at $1,617$ shifted to $1,637$ after the MG adsorption. It was indicated that there was a chemical interaction between the MG molecules and carboxylate groups onto the surface of the almond shell. There are also other peaks shifting from $3,419$ to $3,421\text{ cm}^{-1}$ and $1,049$ to $1,052\text{ cm}^{-1}$, demonstrating that the amine and hydroxyl groups were responsible for the MG adsorption on almond shells.

3.12. Comparison of the almond shell with other sorbents

Comparison of adsorption capacity of different materials on methyl green dye given in results and discussion parts as a Table 8. It can be seen in the table that the adsorption capacity of the almond shell was higher than sepiolite but lower than others. No pre-treatment was applied to the almond shell used in this study to reduce the cost and increase their applicability. For this reason, the adsorption capacity was low.

4. Conclusion

There are some critical results in this investigation. These can be listed as follows: a new adsorbent was discovered for Methyl Green, the optimum process parameters determined by the utilization of a CCD prompting to the maximum percentage removal of Methyl Green molecule from aqueous solution, change of adsorption rate discovered with changing test conditions and reducing the experimental system design time via performing a lesser number of tests.

The almond shells are present in large quantities and waste materials that do not require any further pre-treatment while using it as an adsorbent. Therefore, adsorption experiments on almond shells are an option for removing Methyl Green from aqueous solutions. CCD was applied to find the

Table 8
Comparison adsorption capacity of MG on almond shell with different adsorbents and dyes

Sorbent	q_{\max} (mg/g)	Name of the dye used	Reference
Jute fiber	29.697	Anionic-Azo	[62]
Modified jute fiber	169.49	Aniline	[63]
Biomass fly ash	4.38	Reactive Black 5	[64]
Biomass fly ash	3.65	Reactive Yellow 176	[64]
Fine grinded wheat straw	2.23	Methylene Blue	[65]
Neem (<i>Azadirachta indica</i>) leaf powder	3.67	Methylene Blue	[66]
Coarse grinded wheat straw	3.82	Methylene Blue	[65]
Cashew nut shell	5.311	Methylene Blue	[67]
Almond shell	1.075	Crystal Violet	[22]
Coconut (<i>Cocos nucifera</i>) shell	50.6	Methylene Blue	[68]
Rice husk	4.35	Direct Red 23	[69]
Spent rice biomass	8.3	Methylene blue	[70]
Loofah fibers	18.16	Methylene Green	[61]
Sepiolite	0.09488	Methylene Green	[7]
Amberlite XAD-4 resin	1.157	Methylene Green	[71]
Almond shell	1.1	Methylene Green	This work

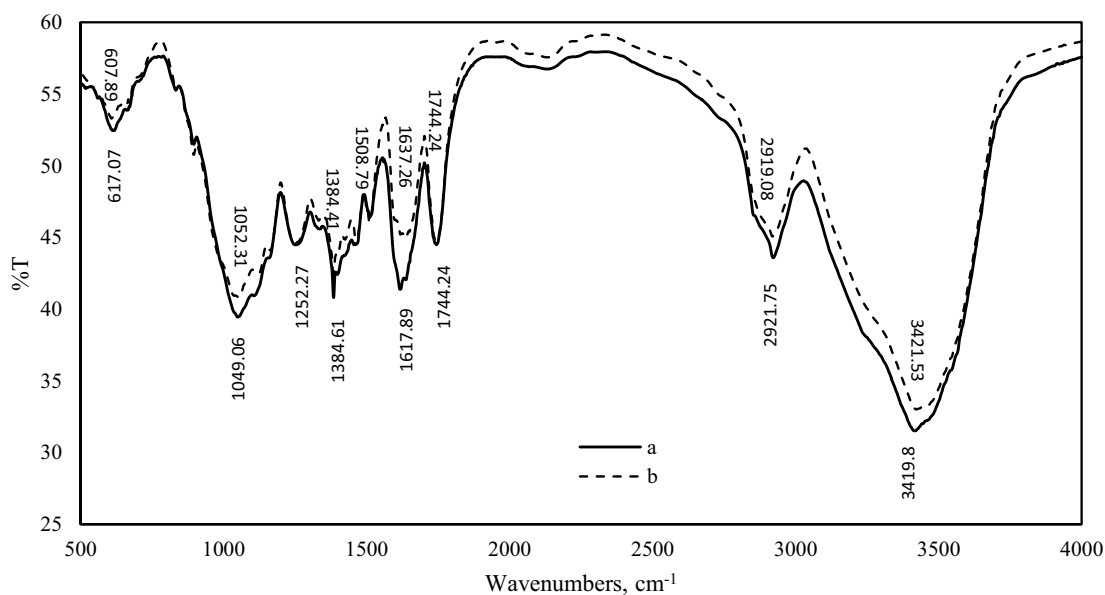


Fig. 15. FTIR spectrum of almond shells (a) before adsorption and (b) after adsorption of MG.

optimum removal conditions through 30 experiments. The optimum values of parameters by CCD were determined as the adsorbent dose of 0.5 g, the initial concentration of 6 ppm, the particle size of 163 μm , and the shaking rate of 200 rpm. The adsorption rate was increased regarding the increasing amounts of the adsorbent, initial concentration, shaking speed, pH, and temperature. The amount of adsorbed dye on almond shells was decreased regarding the increasing particle size of the adsorbent. The Langmuir adsorption isotherm model was perfectly fitted. Methyl Green adsorption rate was performed depending on pseudo-first-order, pseudo-second-order equations, and the adsorption pursued pseudo-second-order kinetic equation. The thermodynamic parameters such as ΔG° , ΔH° , and ΔS° were calculated and found to be -2.878 , 42.12 kJ/mol, and 0.151 kJ/mol K, respectively. The parameters indicate that the adsorption on almond shells was endothermic, spontaneous, and increased randomness at the solid/solution interface, respectively. The outcomes showed that the CCD statistical methodology was a proper instrument to optimize the process parameters for maximized removal effectiveness. The maximum adsorption capacity was found to be 1.1 mg/g. This examination presents almond shells that are an agricultural waste, a new and commercial possibility for Methyl Green adsorption and it well may be utilized to remove cationic dyes in industrial waste streams.

Acknowledgments

This research did not receive any specific grant from funding agencies in the public, commercial, or not-for-profit sectors.

References

- [1] P. Sharma, M.R. Das, Removal of a cationic dye from aqueous solution using graphene oxide nanosheets: investigation of adsorption parameters, *J. Chem. Eng. Data*, 58 (2013) 151–158.
- [2] F. Güzel, H. Saygılı, G.A. Saygılı, F. Koyuncu, Decolorisation of aqueous crystal violet solution by a new nanoporous carbon: equilibrium and kinetic approach, *J. Ind. Eng. Chem.*, 20 (2014) 3375–3386.
- [3] Y. Haik, S. Qadri, A. Gano, S. Ashraf, R. Sawafta, Phase change material for efficient removal of crystal violet dye, *J. Hazard. Mater.*, 176 (2010) 1110–1112.
- [4] Y. Gao, S.Q. Deng, X. Jin, S.L. Cai, S.R. Zheng, W.G. Zhang, The construction of amorphous metal-organic cage-based solid for rapid dye adsorption and time-dependent dye separation from water, *Chem. Eng. J.*, 357 (2019) 129–139.
- [5] A. Kausar, M. Iqbal, A. Javed, K. Aftab, Z.-H. Nazli, H.N. Bhatti, S. Nouren, Dyes adsorption using clay and modified clay: a review, *J. Mol. Liq.*, 256 (2018) 395–407.
- [6] G.O. El-Sayed, Removal of methylene blue and crystal violet from aqueous solutions by palm kernel fiber, *Desalination*, 272 (2011) 225–232.
- [7] G. Rytwo, D. Tropp, C. Serban, Adsorption of diquat, paraquat and methyl green on sepiolite: experimental results and model calculations, *Appl. Clay Sci.*, 20 (2002) 273–282.
- [8] A. Maghni, M. Ghelamallah, A. Benghalem, Sorptive removal of Methyl Green from aqueous solutions using activated bentonite, *Acta Phys. Pol. A*, 132 (2017) 448–450.
- [9] A. Saeed, M. Sharif, M. Iqbal, Application potential of grapefruit peel as dye sorbent: kinetics, equilibrium and mechanism of crystal violet adsorption, *J. Hazard. Mater.*, 179 (2010) 564–572.
- [10] S.M. Alardhi, T.M. Albayati, J.M. Alrubaye, Adsorption of the methyl green dye pollutant from aqueous solution using mesoporous materials MCM-41 in a fixed-bed column, *Heliyon*, 6 (2020) e03253, doi: 10.1016/j.heliyon.2020.e03253.
- [11] T. Aysu, M.M. Küçük, Removal of crystal violet and methylene blue from aqueous solutions by activated carbon prepared from *Ferula orientalis*, *Int. J. Environ. Sci. Technol.*, 12 (2015) 2273–2284.
- [12] R. Ahmad, Studies on adsorption of crystal violet dye from aqueous solution onto coniferous pinus bark powder (CPBP), *J. Hazard. Mater.*, 171 (2009) 767–773.
- [13] A.S. Sartape, A.M. Mandhare, V.V. Jadhav, P.D. Raut, M.A. Anuse, S.S. Kolekar, Removal of malachite green dye from aqueous solution with adsorption technique using *Limonia acidissima* (wood apple) shell as low cost adsorbent, *Arabian J. Chem.*, 10 (2017) S3229–S3238.
- [14] F. Marahel, Adsorption of hazardous methylene green dye from aqueous solution onto tin sulfide nanoparticles loaded

- activated carbon: isotherm and kinetics study, Iran. J. Chem. Chem. Eng., 38 (2019) 129–142.
- [15] J. Gülen, B. Akin, M. Özgür, Ultrasonic-assisted adsorption of methylene blue on sumac leaves, Desal. Water Treat., 57 (2016) 9286–9295.
- [16] S.K. Low, M.C. Tan, Dye adsorption characteristic of ultrasound pre-treated pomelo peel, J. Environ. Chem. Eng., 6 (2018) 3502–3509.
- [17] B.H. Hameed, Equilibrium and kinetic studies of methyl violet sorption by agricultural waste, J. Hazard. Mater., 154 (2008) 204–212.
- [18] S.M. Alardhi, J.M. Alrubaye, T.M. Albayati, Adsorption of methyl green dye onto MCM-41: equilibrium, kinetics and thermodynamic studies, Desal. Water Treat., 179 (2020) 323–331.
- [19] Almond Global Production and Top Producing Countries – Tridge, (n.d.). Available at: <https://www.tridge.com/intelligences/almond-in-shell/production> (accessed March 10, 2021).
- [20] Almond Production in Turkey - Tridge, (n.d.). Available at: <https://www.tridge.com/intelligences/almond-in-shell/TR/production> (accessed March 10, 2021).
- [21] M. Ishaq, F. Javed, I. Amad, H. Ullah, F. Hadi, S. Sultan, Adsorption of Crystal violet dye from aqueous solutions onto low-cost untreated and NaOH treated almond shell, Iran. J. Chem. Chem Eng., 35 (2016) 97–106.
- [22] A. Goksu, M.K. Tanaydin, Adsorption of hazardous crystal violet dye by almond shells and determination of optimum process conditions by Taguchi method, Desal. Water Treat., 88 (2017) 189–199.
- [23] A. Göksu, M.K. Tanaydin, Determination of optimum conditions of crystal violet dye adsorption on almond shells, AIP Conf. Proc., 1813(2017) 020114-1–020114-3 doi: 10.1063/1.4981762.
- [24] K. Saeed, M. Ishaq, S. Sultan, I. Ahmad, Removal of methyl violet 2-B from aqueous solutions using untreated and magnetite-impregnated almond shell as adsorbents, Desal. Water Treat., 57 (2016) 13484–13493.
- [25] R.F. Gunst, R.H. Myers, D.C. Montgomery, Response surface methodology: process and product optimization using designed experiments, Technometrics, 38 (2006) 285.
- [26] N. Kataria, V.K.K. Garg, Optimization of Pb(II) and Cd(II) adsorption onto ZnO nanoflowers using central composite design: isotherms and kinetics modelling, J. Mol. Liq., 271 (2018) 228–239.
- [27] A. Morshedi, M. Akbarian, Application of response surface methodology: design of experiments and optimization: a mini review, Indian J. Fundam. Appl. Life Sci., 4 (2014) 2231–6345.
- [28] B. Sadhukhan, N.K. Mondal, S. Chattoraj, Optimisation using central composite design (CCD) and the desirability function for sorption of methylene blue from aqueous solution onto *Lemna major*, Karbala Int. J. Mod. Sci., 2 (2016) 145–155.
- [29] A. Hassani, M. Kiranşan, R. Darvishi Cheshmeh Soltani, A. Khataee, S. Karaca, Optimization of the adsorption of a textile dye onto nanoclay using a central composite design, Turk. J. Chem., 39 (2015) 734–749.
- [30] F. Deniz, S.D. Saygideger, Investigation of adsorption characteristics of Basic Red 46 onto gypsum: equilibrium, kinetic and thermodynamic studies, Desalination, 262 (2010) 161–165.
- [31] Z. Salahshoor, A. Shahbazi, Modeling and optimization of cationic dye adsorption onto modified SBA-15 by application of response surface methodology, Desal. Water Treat., 57 (2016) 13615–13631.
- [32] P. Monash, G. Pugazhenth, Adsorption of crystal violet dye from aqueous solution using mesoporous materials synthesized at room temperature, Adsorption, 15 (2009) 390–405.
- [33] L.S. Oliveira, A.S. Franca, T.M. Alves, S.D.F. Rocha, Evaluation of untreated coffee husks as potential biosorbents for treatment of dye contaminated waters, J. Hazard. Mater., 155 (2008) 507–512.
- [34] V. Ponnusami, V. Gunasekar, S.N. Srivastava, Kinetics of methylene blue removal from aqueous solution using gulmohar (*Delonix regia*) plant leaf powder: multivariate regression analysis, J. Hazard. Mater., 169 (2009) 119–127.
- [35] H.B. Senturk, D. Ozdes, C. Duran, Biosorption of Rhodamine 6G from aqueous solutions onto almond shell (*Prunus dulcis*) as a low cost biosorbent, Desalination, 252 (2010) 81–87.
- [36] T. Mekhalif, K. Guediri, A. Reffas, D. Chebli, A. Bouguettoucha, A. Amrane, Effect of acid and alkali treatments of a forest waste, *Pinus brutia* cones, on adsorption efficiency of methyl green, J. Dispersion Sci. Technol., 38 (2017) 463–471.
- [37] I.A.W. Tan, A.L. Ahmad, B.H. Hameed, Adsorption isotherms, kinetics, thermodynamics and desorption studies of 2,4,6-trichlorophenol on oil palm empty fruit bunch-based activated carbon, J. Hazard. Mater., 164 (2009) 473–482.
- [38] B. Nandi, A. Goswami, M. Purkait, Removal of cationic dyes from aqueous solutions by kaolin: kinetic and equilibrium studies, Appl. Clay Sci., 42 (2009) 583–590.
- [39] C.A.P. Almeida, N.A. Debacher, A.J. Downs, L. Cottet, C.A.D. Mello, Removal of methylene blue from colored effluents by adsorption on montmorillonite clay, J. Colloid Interface Sci., 332 (2009) 46–53.
- [40] S. Senthilkumar, P. Kalaamani, C. Subraam, Liquid phase adsorption of Crystal violet onto activated carbons derived from male flowers of coconut tree, J. Hazard. Mater., 136 (2006) 800–808.
- [41] S. Çoruh, F. Geyikçi, E. Kılıç, U. Çoruh, The use of NARX neural network for modeling of adsorption of zinc ions using activated almond shell as a potential biosorbent, Bioresour. Technol., 151 (2014) 406–410.
- [42] S. Babel, T.A. Kurniawan, Low-cost adsorbents for heavy metals uptake from contaminated water: a review, J. Hazard. Mater., 97 (2003) 219–243.
- [43] R. Kumar, R. Ahmad, Biosorption of hazardous crystal violet dye from aqueous solution onto treated ginger waste (TGW), Desalination, 265 (2011) 112–118.
- [44] F. Doulati Ardejani, K. Badii, N.Y. Limaee, S.Z. Shafaei, A.R. Mirhabibi, Adsorption of Direct Red 80 dye from aqueous solution onto almond shells: effect of pH, initial concentration and shell type, J. Hazard. Mater., 151 (2008) 730–737.
- [45] Y. Bulut, Z. Tez, Adsorption studies on ground shells of hazelnut and almond, J. Hazard. Mater., 149 (2007) 35–41.
- [46] K.M. Parida, A.C. Pradhan, Removal of phenolic compounds from aqueous solutions by adsorption onto manganese nodule leached residue, J. Hazard. Mater., 173 (2010) 758–764.
- [47] N. Ertugay, Basic Violet 10 (BV10) removal from aqueous solutions using sawdust of *Swietenia mahagoni* (Mahogany trees): adsorbent characterization, adsorption isotherm, kinetics, and thermodynamic studies, Desal. Water Treat., 57 (2016) 12335–12349.
- [48] Ö. Gerçel, H.F. Gerçel, A.S. Kopalal, Ü.B. Ögütveren, Removal of disperse dye from aqueous solution by novel adsorbent prepared from biomass plant material, J. Hazard. Mater., 160 (2008) 668–674.
- [49] C. Duran, D. Ozdes, A. Gundogdu, H.B. Senturk, Kinetics and isotherm analysis of basic dyes adsorption onto almond shell (*Prunus dulcis*) as a low cost adsorbent, J. Chem. Eng. Data, 56 (2011) 2136–2147.
- [50] C. Varlikli, V. Bekiari, M. Kus, N. Boduroglu, I. Oner, P. Lianos, G. Lyberatos, S. Icli, Adsorption of dyes on Sahara desert sand, J. Hazard. Mater., 170 (2009) 27–34.
- [51] F. Akbal, Adsorption of basic dyes from aqueous solution onto pumice powder, J. Colloid Interface Sci., 286 (2005) 455–458.
- [52] Ö. Gerçel, A. Özcan, A.S. Özcan, H.F. Gerçel, Preparation of activated carbon from a renewable bio-plant of *Euphorbia rigida* by H₂SO₄ activation and its adsorption behavior in aqueous solutions, Appl. Surf. Sci., 253 (2007) 4843–4852.
- [53] Y. Li, Q. Du, X. Wang, P. Zhang, D. Wang, Z. Wang, Y. Xia, Removal of lead from aqueous solution by activated carbon prepared from *Enteromorpha prolifera* by zinc chloride activation, J. Hazard. Mater., 183 (2010) 583–589.
- [54] L. Wang, J. Zhang, R. Zhao, Y. Li, C. Li, C. Zhang, Adsorption of Pb(II) on activated carbon prepared from *Polygonum orientale* Linn.: kinetics, isotherms, pH, and ionic strength studies, Bioresour. Technol., 101 (2010) 5808–5814.
- [55] F.C. Wu, R.L. Tseng, R.S. Juang, Comparisons of porous and adsorption properties of carbons activated by steam and KOH, J. Colloid Interface Sci., 283 (2005) 49–56.

- [56] B.N. Estevinho, E. Ribeiro, A. Alves, L. Santos, A preliminary feasibility study for pentachlorophenol column sorption by almond shell residues, *Chem. Eng. J.*, 136 (2008) 188–194.
- [57] P. Sharma, B.K. Saikia, M.R. Das, Removal of methyl green dye molecule from aqueous system using reduced graphene oxide as an efficient adsorbent: kinetics, isotherm and thermodynamic parameters, *Colloids Surf., A*, 457 (2014) 125–133.
- [58] S.D. Khattri, M.K. Singh, Removal of malachite green from dye wastewater using neem sawdust by adsorption, *J. Hazard. Mater.*, 167 (2009) 1089–1094.
- [59] R. Ahmad, R. Kumar, Adsorption studies of hazardous malachite green onto treated ginger waste, *J. Environ. Manage.*, 91 (2010) 1032–1038.
- [60] A.K. Kushwaha, N. Gupta, M.C. Chattopadhyaya, Removal of cationic methylene blue and malachite green dyes from aqueous solution by waste materials of *Daucus carota*, *J. Saudi Chem. Soc.*, 18 (2014) 200–207.
- [61] X. Tang, Y. Li, R. Chen, F. Min, J. Yang, Y. Dong, Evaluation and modeling of methyl green adsorption from aqueous solutions using loofah fibers, *Korean J. Chem. Eng.*, 32 (2014) 125–131.
- [62] A. Roy, S. Chakraborty, S.P. Kundu, B. Adhikari, S.B. Majumder, Adsorption of anionic-azo dye from aqueous solution by lignocellulose-biomass jute fiber: equilibrium, kinetics, and thermodynamics study, *Ind. Eng. Chem. Res.*, 51 (2012) 12095–12106.
- [63] D.W. Gao, Q. Hu, H. Pan, J. Jiang, P. Wang, High-capacity adsorption of aniline using surface modification of lignocellulose-biomass jute fibers, *Bioresour. Technol.*, 193 (2015) 507–512.
- [64] P. Pengthamkeerati, T. Satapanajaru, O. Singchan, Sorption of reactive dye from aqueous solution on biomass fly ash, *J. Hazard. Mater.*, 153 (2008) 1149–1156.
- [65] F. Batzias, D. Sidiras, E. Schroeder, C. Weber, Simulation of dye adsorption on hydrolyzed wheat straw in batch and fixed-bed systems, *Chem. Eng. J.*, 148 (2009) 459–472.
- [66] K.G. Bhattacharya, A. Sharma, Kinetics and thermodynamics of Methylene Blue adsorption on Neem (*Azadirachta indica*) leaf powder, *Dyes Pigm.*, 65 (2005) 51–59.
- [67] P. Senthil Kumar, R.V. Abhinaya, K. Gayathri Lashmi, V. Arthi, R. Pavithra, V. Sathyaselvabala, S. Dinesh Kirupha, S. Sivanesan, Adsorption of methylene blue dye from aqueous solution by agricultural waste: equilibrium, thermodynamics, kinetics, mechanism and process design, *Colloid J.*, 73 (2011) 651–661.
- [68] A.H. Jawad, A.S. Abdulhameed, M.S. Mastuli, Acid-fractionalized biomass material for methylene blue dye removal: a comprehensive adsorption and mechanism study, *J. Taibah Univ. Sci.*, 14 (2020) 305–313.
- [69] O. Abdelwahab, A. El Nemr, A. Khaled, Use of rice husk for adsorption of direct dyes from aqueous solution: a case study of direct F. Scarlet, Egypt. *J. Aquat. Res.*, 31 (2005) 1–11.
- [70] M.S.U. Rehman, I. Kim, J.I. Han, Adsorption of methylene blue dye from aqueous solution by sugar extracted spent rice biomass, *Carbohydr. Polym.*, 90 (2012) 1314–1322.
- [71] L.G.T. dos Reis, N.F. Robaina, W.F. Pacheco, R.J. Cassella, Separation of Malachite Green and Methyl Green cationic dyes from aqueous medium by adsorption on Amberlite XAD-2 and XAD-4 resins using sodium dodecylsulfate as carrier, *Chem. Eng. J.*, 171 (2011) 532–540.